

Synthesis, cytotoxic activity, DNA binding and molecular docking studies of novel 9-anilinothiazolo[5,4-*b*]quinoline derivatives

Francisco J. Reyes-Rangel¹ · A. Kémish López-Rodríguez¹ ·
Laura V. Pastrana-Cancino² · Marco. A. Loza-Mejía¹ · José D. Solano³ ·
Rogelio Rodríguez-Sotres² · Alfonso Lira-Rocha¹ 

Received: 10 February 2016 / Accepted: 22 August 2016
© Springer Science+Business Media New York 2016

Abstract Novel thiazolo[5,4-*b*]quinoline derivatives were prepared with or without a (2-(azacycloalkyl)ethyl)amino substituent at the 2-position. The effect of the substituent at 2-position on cytotoxic activity, DNA-intercalation and cytotoxic properties were evaluated. Substituents at 2-position bearing an aliphatic amine favored cytotoxicity, while removal of these substituents resulted in low or negligible cytotoxic properties. Additionally, the *in silico* predicted binding mode of the novel compounds into DNA correlated with the experimental intercalation data. These results suggest a strong influence of the substituent at 2-position on the DNA intercalation properties.

Keywords Thiazolo[5,4-*b*]quinoline · Cytotoxic activity · DNA intercalators · Molecular docking

Introduction

Cancer is still a worldwide health problem, affecting both developing and developed countries. While several strategies have been proposed for the treatment of cancer, the small-molecule approach is still an important alternative (Hoelder et al., 2012). In this case, the 9-anilinoacridine derivatives (1, Fig. 1) have proven to be clinically efficacious and extensively studied as antitumor agents targeting DNA-topoisomerase II (Siu and Pommier, 2013; Lindsey et al., 2014; Demecunynck et al., 2001). One of these derivatives, Amsacrine 2 (*m*-AMSA), has been used for the treatment of leukemia and lymphoma (Denny, 1995, 2002). In order to overcome the mechanism of resistance and to increase the selectivity of drugs towards cancer cells, bioisosteric replacement of a benzene moiety in the acridine nucleus has led to cytotoxic novel compounds, such as thiazolo[5,4-*b*]quinoline 3 (Rodríguez-Loaiza et al., 2004;

Electronic supplementary material The online version of this article (doi:10.1007/s00044-016-1718-4) contains supplementary material, which is available to authorized users.

✉ Alfonso Lira-Rocha
lira@unam.mx

¹ Departamento de Farmacia, Facultad de Química, Universidad Nacional Autónoma de México, Cd. Universitaria, 04510 Coyoacán, México, Mexico

² Departamento de Bioquímica, Facultad de Química, Universidad Nacional Autónoma de México, Cd. Universitaria, 04510 Coyoacán, México, Mexico

³ Departamento de Biología, Facultad de Química, Universidad Nacional Autónoma de México, Cd. Universitaria, 04510 Coyoacán, México, Mexico

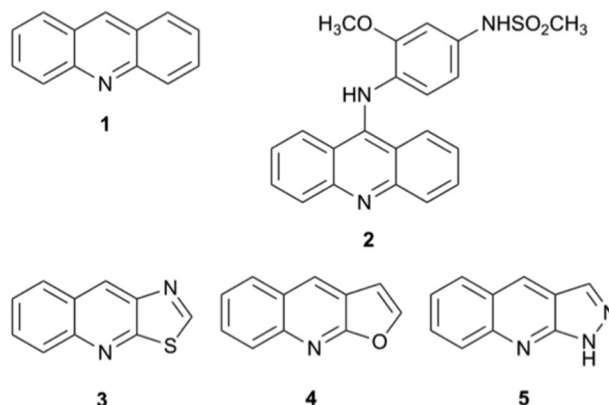
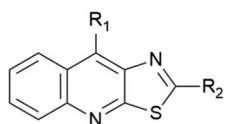
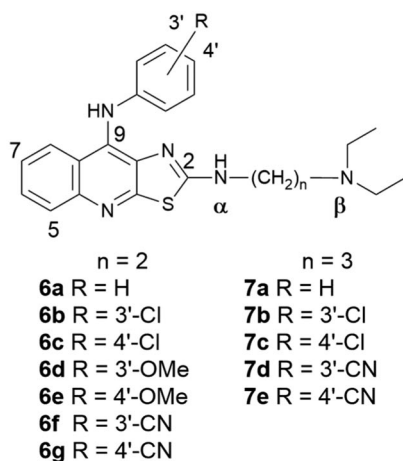


Fig. 1 Chemical structure of acridine 1, *m*-AMSA 2 and some tricyclic templates



- 6h** R₁ = -HN-C₆H₄-3'-CONH(CH₂)₂N(CH₂CH₃)₂ R₂ = -SCH₃
6i R₁ = Cl R₂ = -NH(CH₂)₂N(CH₂CH₃)₂
6j R₁ = -NH(CH₂)₂N(CH₂CH₃)₂ R₂ = -SCH₃

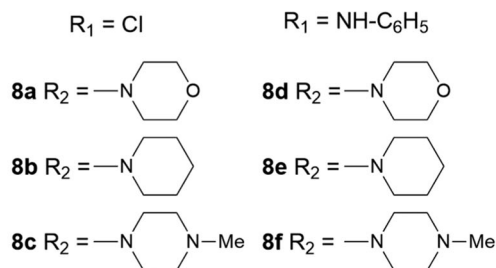


Fig. 2 Chemical structure of thiazolo[5,4-*b*]quinoline derivatives previously reported (Loza-Mejía et al., 2009)

Loza-Mejía et al., 2008; González-Sánchez et al., 2011), furo[2,3-*b*]quinoline **4** (Chen et al., 2004), and pyrazolo[3,4-*b*]quinoline **5** derivatives among others (Chen et al., 2005).

In previous reports, we described the synthesis, cytotoxic activity and DNA-topoisomerase II inhibition properties of several derivatives of thiazolo[5,4-*b*]quinoline as potential anticancer agents (Loza-Mejía et al., 2009). In these reports, a diethylaminoethylamino group (series **6**) or a 3-(diethylamino)propyl-amino (series **7**) substituent at 2-position of the thiazoloquinoline nucleus was found to correlate with increased cytotoxicity regardless of the substitution pattern in the 9-anilino ring (Fig. 2). In addition, compounds with a two-methylene chain were less cytotoxic than their three-methylene chain counterparts. The influence of the side chain conformation at 2-position was probed with several saturated heterocyclic analogs (series **8**). These compounds were less cytotoxic than the corresponding open chain analogs, indicating a flexibility requirement at the lateral

chain. This point to a strong influence of the substitution pattern at 2-position on cytotoxicity.

In the present work, two new miniseries of thiazolo[5,4-*b*]quinoline derivatives were prepared. In the first series, a ring of five or six members was incorporated at the end of the side chain (series **15**) to anchor its β -nitrogen. In the second series, the substituent at 2-position was removed by the displacement of a sulfonyl group (series **16**). The cytotoxic activity of these novel compounds was evaluated in some tumor cell lines. The results confirm the significance of the substituent at 2-position. The primary target of thiazolo[5,4-*b*]quinoline derivatives has not been confirmed experimentally, but the DNA is the biological target of *m*-AMSA and others 9-anilinoacridines. Therefore, we include here the intercalating properties of the new compounds from experimental data and predictions of the binding mode of these novel compounds, based on *in silico* molecular docking studies.

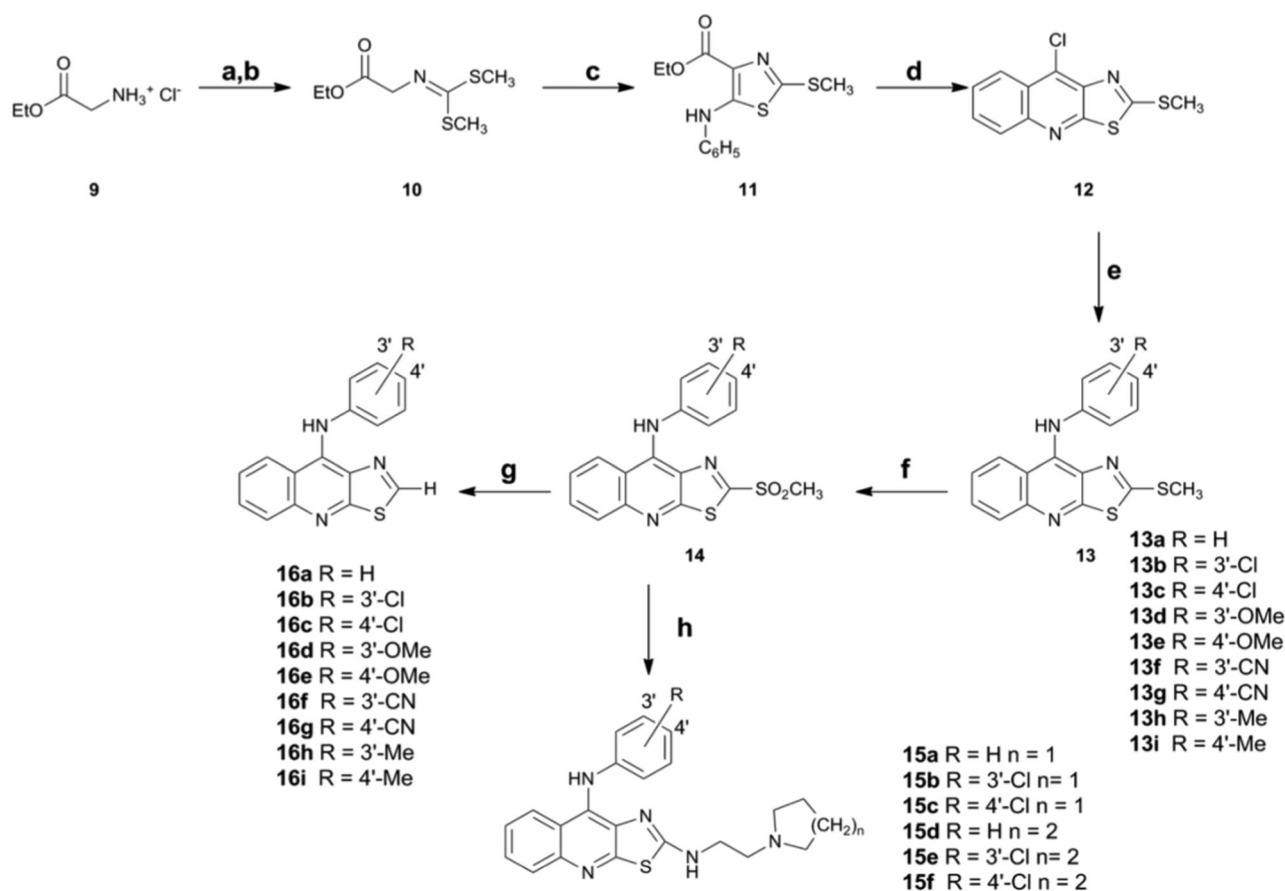
Results and discussion

Chemistry

Novel compounds were obtained by a divergent synthesis based on a methodology already reported with some modifications (Loza-Mejía et al., 2009) Scheme 1.

Compound **10** was prepared using CHCl₃ instead of DMSO, as a reaction solvent, and dimethyl sulfate instead of methyl iodide as an alkylating agent. In our experience, the displacement of a methylthio group present in a thiazole ring can be accomplished directly by a nucleophilic aromatic substitution reaction, but the yield can be improved by the previous transformation to the corresponding sulfonyl derivative. We have previously reported this last reaction with H₂O₂ in AcOH for 24 h at room temperature, but in some cases further purification procedures were required, with a decrease in the yield of the sulfonyl compound. Among the reported oxidizing agents, hydrogen peroxide is an environmentally friendly substance and its oxidant properties can be enhanced by some Lewis acid metal catalysts (He et al., 2012; Sato et al., 2001). Thus, the oxidation of compounds **13–14** was accomplished by H₂O₂ and catalytic amounts of Na₂WO₄ · 2H₂O to afford the corresponding sulfonyl derivative in good yield. This procedure cuts down reaction times (30 min) and facilitates the work-up reaction. From this step onwards, the synthesis becomes divergent. The substitution of the sulfonyl group with the corresponding amine was carried out in DMF to render **15** series compounds.

On the other hand, several methodologies have been reported for the elimination of a methylthio group attached to a heterocyclic ring; for instance, Baldwin et al. (1980)



Scheme 1 a $\text{CS}_2/\text{TEA}/\text{CHCl}_3/(\text{CH}_3)_2\text{SO}_4$; b $(\text{CH}_3)_2\text{SO}_4/\text{K}_2\text{CO}_3/\text{Me}_2\text{CO}$; c 1. *t*-BuOK/THF 2. $\text{C}_6\text{H}_5\text{-NCS}$; d PPA/ POCl_3 130 °C; e $\text{NH}_2\text{-C}_6\text{H}_4\text{-R}$; f $\text{Na}_2\text{WO}_4/\text{AcOH}/\text{H}_2\text{O}_2$; g $\text{NaBH}_4/\text{EtOH}$; h $\text{NH}_2\text{-CH}_2\text{CH}_2\text{-N}(\text{CH}_2\text{CH}_2)_2$ or $\text{NH}_2\text{-CH}_2\text{CH}_2\text{-N}(\text{CH}_2\text{CH}_2)_2\text{CH}_2/\text{DMF}$

reported the elimination of the mentioned group attached at 2-position of a thiazole ring using Zn/HCl 3N. Other authors have reported this transformation by treating furan derivatives with Raney Ni in EtOH (Herrera et al., 2006; Yin et al., 2008). In the case of series **16**, the removal of this substituent from **13** with Zn/HCl was unsuccessful. Previous reports concerning the hydrogenolytic removal of halogen at 2-position of the thiazole ring prompted us to apply this methodology by using sodium borohydride as a reducing agent (Kerdesky and Seif, 1995); however, more efficient desulfurization processes have been accomplished by the previous transformation of the thioether group to the corresponding sulfone derivative (Zumbrunn, 1998). Hence, the corresponding sulfonyl derivative **14** was treated with NaBH_4 in THF, but the yields were about 40 % in all cases. Yields improved with the use of absolute EtOH as solvent (approx 70 %). However, all of these three strategies failed to remove the methylthio group from compounds **11** and **12**.

The structures of novel compounds were determined by IR, ^1H NMR and HRMS. For example, compound 9-[(3-methoxyphenyl)amino]thiazolo[5,4-*b*]quinoline **16d** with

an quasi-molecular ion peak M^+ at m/z 307.0774 was in good agreement with the molecular formula $\text{C}_{17}\text{H}_{13}\text{N}_3\text{SO}$. In the IR spectrum, the typical bands for a sulfonyl group (1317 and 1146 cm^{-1}) were absent. The NH band was observed at 3120 cm^{-1} , as well as the aromatic bands at 1595, 1571, 1543, 1503, 1476 and the vibration C–S at 764 cm^{-1} . In the ^1H NMR spectrum, the simple signal observed at 9.40 ppm was assigned to the Ar–NH–Ar proton while the other simple signal at 9.22 ppm was attributed to the proton at 2-position. This chemical shift is in agreement with a previous report of Dercitin spectral data, an acridine alkaloid fused to a thiazole ring (Gunawardana et al., 1988). The proton-proton coupling signals for H-2 were absent in the NOESY experiment, providing evidence for the absence of spatial proximity of other protons. Quinoline proton signals appeared at 8.29 and 7.87 ppm and corresponded to H-8 and H-5, respectively, while H-6 and H-7 protons signals were observed at 7.75 and 7.49 ppm, respectively. The multiple signals in the range of 6.60–6.58 ppm were assigned to H-2', H-4', H-6', and the signal at 7.11 ppm was assigned to H-5'. The ^{13}C NMR spectrum was used to

verify the integrity of the molecule. The spectrum revealed 17 carbon-resonances, interpreted from DEPT experiment data as seven quaternary, nine methine, and one methyl carbons. The presence of the thiazole ring was supported by the resonance signals at 160.7 (C2), 141.1 (C3a) and 133.1 (C9a) ppm. In addition, the absence of a signal at 14.5 ppm, normally present in the spectrum of several methylthio derivatives (Loza-Mejía et al., 2008), indicated the successful removal of this substituent at 2-position. The assignment of all signals is reported in the experimental section.

Cytotoxic activity

The cell lines used in the present study were: one cervical cancer line (HeLa), two colorectal cancer cell lines (SW-480 and SW-620) and one leukemic cell line (K-562). The cytotoxic assays were carried out using the methodology already described (Quintero et al., 1999). The cytotoxic

Table 1 Cytotoxic activity of already reported compounds^a (series **6** and **13**) and novel compounds (series **15** and **16**) (IC₅₀ μM)

Compound	HeLa	SW-480	SW-620	K-562
6a ^a	15.96	37.7	21.6	16.8
6b ^a	9.12	14.33	17.78	12.19
6c ^a	10.16	12.56	12.20	7.26
13a ^a	>200	>200	>200	>200
13b ^a	69.37	110.69	129.73	80.26
13c ^a	123.86	>200	149.95	79.45
13d ^a	25.34	66.65	26.58	22.17
13e ^a	>200	>200	110.8	72.2
13f ^a	7.75	28.68	43.75	8.01
15a	27.81	29.1	31.58	24.11
15b	14.64	15.42	14.37	5.69
15c	17.46	26.51	13.47	19.48
15d	32.28	26.7	20.13	21.25
15e	12.06	12.75	18.12	10.62
15f	14.42	18.42	11.6	7.38
16a	ND	ND	ND	ND
16b	ND	ND	ND	ND
16c	ND	ND	ND	ND
16d	27.2	73.9	73.6	23.6
16e	30.8	ND	ND	41.8
16f	ND	ND	ND	ND
16g	ND	ND	ND	ND
16h	85.8	56.4	83.2	4.5
16i	ND	ND	ND	33.7
<i>m</i> -AMSA	14.63	19.75	16.73	9.84

ND no cytotoxicity at the highest concentration tested (100 μM)

^a Data taken from Loza-Mejía et al., 2009

activity data of previously reported compounds and novel compounds are shown in Table 1.

By comparison of their activity profiles, compounds **15a–15c** are slightly less active than compounds **6a–6c**, whereas there is no any significant difference between the activity of compounds **6a–6c** and **15d–15f**. Compounds **15d–15f** are slightly more active than compounds **15a–15c**. Apparently, a strainless tertiary amine at the β-nitrogen atom of the side chain has a positive effect on cytotoxicity. However, according to the results of molecular docking study, the most cytotoxic compounds had high binding score in their protonated state (*vide infra*). The theoretical pKa values of compounds **6a**, **15a** and **15d** (non-chlorinated members of the corresponding miniseries) were calculated using web calculator software. (Marvin 5.4.0.1, 2010, <http://www.chemaxon.com>), and the pKa value for the most active compound **6a** was 9.16, whereas for compounds **15a** and **15d** were 8.55 and 8.43, respectively (>90 % protonated state for all three molecules, at pH 7.0). Thus, the basic properties of the side chain may influence the efficacy of the cytotoxic activity of these compounds and further studies are in course in order to evaluate this possibility.

On the other hand, the halo derivatives of both series showed activity improvements. According to these facts, the cytotoxic activity is also modulated by the substitution pattern in the anilino ring (Loza-Mejía et al., 2008).

In the **16** series, the removal of the substituent at 2-position reduces or eliminates the cytotoxic activity (Table 1, compare series **13** with series **16**), except for compounds **16d**, **16e**, and **16h**, which were active on K-562 cell line and only slightly active on HeLa cells.

In order to make a more graphical comparison of the cytotoxic potency of compounds for a given cell line, a cytotoxic index (*CtxI*) was obtained by dividing the IC₅₀ of Amsacrine by that of the compound, for the given cell line. A *CtxI* above one is indicative of cytotoxic compounds more potent than Amsacrine. The *CtxI* may also be used to identify those cell lines with a higher sensitivity to the cytotoxic effect of the compounds under analysis. The *CtxI* values for series **6** were obtained by using the *m*-AMSA value previously reported (Loza-Mejía et al., 2009).

As shown in Fig. 3, no compound is more cytotoxic than *m*-AMSA against HeLa cells (panel A) with exception of compound **15e**. In contrast, some compounds of the series **6** and **15** (Fig. 3, panels B and D) are more cytotoxic than *m*-AMSA, against SW-480 and K-562 cell lines. A common feature of these compounds is a dialkylaminoalkylamino chain at the 2-position.

DNA binding (Ethidium bromide displacement)

Apparent DNA intercalation constants were determined by a conventional method based on the quenching of the

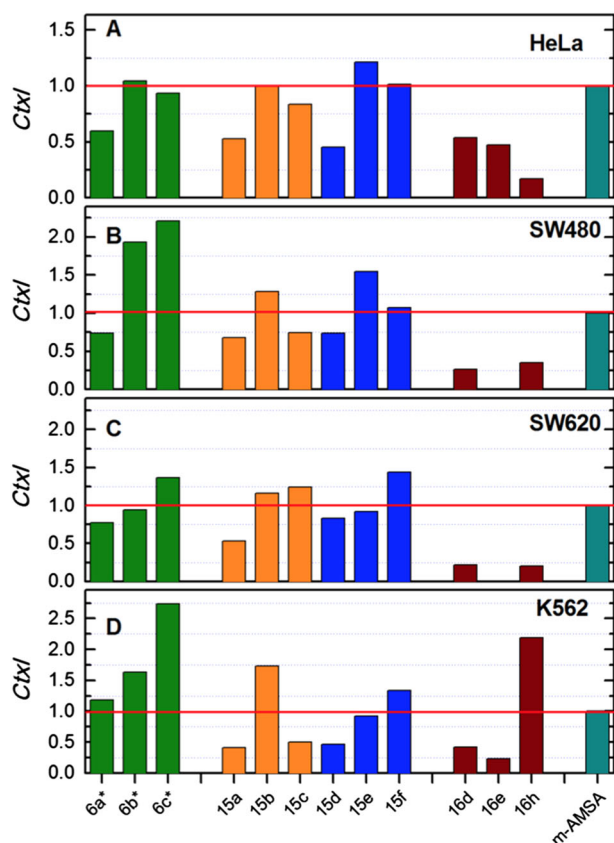


Fig. 3 Cytotoxicity index for some compounds of series **6**, **15** and **16**

fluorescence of the ethidium bromide-DNA complex, as previously described (McConnaughie and Jenkins, 1995). DNA has been considered as the target of several antitumor agents. In a previous report, we determined the DNA intercalating properties of several thiazolo[5,4-*b*]quinoline derivatives (Loza-Mejía et al., 2008).

According to data in Table 2, compounds with an ethylenediamine group (series **15** and compound **6a**) displace more ethidium bromide than 2-methylthio derivatives (Higher Q_{\max}). However, an inverse tendency was observed for the binding affinity values (Q_{50}), i.e. less active compounds bound to DNA tighter than more active ones. It is clear that the compounds with a chlorine atom displaced ethidium bromide from more sites (Higher Q_{\max}) than the compounds without this atom; and this trend roughly correlates with the cytotoxic data.

On the other hand, it is interesting that the Q_{\max} values for the compounds without a methylthio group are higher than those of 2-methylthio derivatives and the Q_{50} values for the first ones also are higher. This implies that multiples sites in the DNA are occupied by the compounds of series **16** with low binding affinity (low “selectivity”) and this could explain their low or null cytotoxic activity. Only the compounds **16d** and **16e** showed significant activity.

Table 2 Apparent constants for ethidium bromide displacement from DNA of already reported compounds^a (series **13**) and novel compounds (series **15** and **16**)

Compound	Q_{\max}^b	Q_{50}^c	Q_{\max}/Q_{50}
6a ^a	70.86	16.86	4.20
13a ^a	4.17	13.62	0.31
13b ^a	2.60	1.29	2.00
13c ^a	1.84	2.19	0.84
13d ^a	6.65	3.71	1.79
13e ^a	3.73	9.48	0.39
13f ^a	7.84	11.54	0.68
15a	39.24	15.08	2.60
15b	50.62	37.18	1.36
15c	77.39	53.56	1.44
15d	24.88	8.10	3.07
15e	50.05	33.87	1.48
15f	30.42	22.17	1.37
16a	35.10	28.22	1.24
16b	20.64	15.93	1.30
16d	20.66	9.42	2.19
16e	23.90	11.11	2.15
16f	19.03	9.09	2.09
m-AMSA	47.79	7.36	6.49

^a Data taken from Loza-Mejía et al., 2008

^b Maximum quenching

^c Concentration to give 50 % quenching of fluorescence of bound ethidium bromide (μM). Values are the mean of three experiments

These two compounds showed a good apparent efficiency index (ratio Q_{\max}/Q_{50}). It is true that compounds with an ethylenediamine group also exhibit high Q_{50} values, and thus low intercalation efficiency index, and yet these compounds exhibit high cytotoxicity. These data indicates that intercalating properties are not enough to predict the cytotoxicity of these compounds, and clearly additional properties ought to be considered (Xiao et al., 2005).

Docking studies

In order to determine the binding mode of action of the novel compounds, rigid/flexible molecular docking studies with DNA- N^{α} -(9-acridinoyl)-tetraarginine complex crystal (PDB code:1G3X) (Malinina et al., 2002) were performed. Antitumor activity of DNA-intercalators is generally associated with strong DNA-binding and long drug residence times at individual sites. The binding energy values for novel compounds and some previously reported are listed in the Table 3. The tricyclic system was intercalated between the base pairs of DNA, and the anilino group was always oriented into the minor groove. In all of the cases analyzed

Table 3 Binding free energy values for already reported compounds and novel compounds

Compound	DNA binding energy (ΔG) from molecular docking force field (kcal mol ⁻¹)	DNA binding energy (ΔH_f) from PM7 calculations (kcal mol ⁻¹)
6a	-10.03	-65.12
6b	-10.81	-66.72
6c	-10.31	-76.06
13a	-8.51	-39.04
13b	-8.79	-47.02
13c	-8.65	-45.61
15a	-10.52	-65.32
15b	-11.19	-71.28
15c	-10.20	-62.17
15d	-10.66	-63.43
15e	-10.79	-72.85
15f	-11.21	-73.65
16a	-7.81	-40.75
16b	-8.32	-47.89
16c	-8.01	-47.88
16d	-8.08	-42.42
16e	-7.66	-45.01
16f	-8.22	-42.21
16g	-7.87	-44.20
16h	-8.08	-44.38
16i	-7.98	-42.96

here, the thiazole ring was stacked in between thymine bases (T619 and T620), with the exception of compounds **13a** and **13b**, in which it was stacked in between adenine bases (A605 and A606). The energy values corresponding to the compounds with a side-chain at 2-position were the lowest (higher binding affinity) and directly correlated with their Q_{\max} values and cytotoxicity.

The principal interactions observed for the compounds of series **15** were π - π stacking, hydrogen bonding and salt bridge formation. A salt bridge was consistently formed between the tertiary amino group and phosphate oxygen (O620 or O619) of the DNA backbone (Fig. 4). The orientation adopted by the tricyclic system in the docked complex renders an optimum overlap with the DNA base pairs (Fig. 5).

On the other hand, compounds lacking the methylthio group were expected to have higher affinity for DNA than the compounds bearing this group. However, the experimental data indicated an opposite trend, because on average, series **16** showed a 2-times higher Q_{50} value than series **13**. From the analysis of the docked complexes, compounds bearing a methylthio group were predicted to dock into DNA with a better overlap of the thiazoloquinoline nucleus and the DNA base pairs; whereas the compounds without

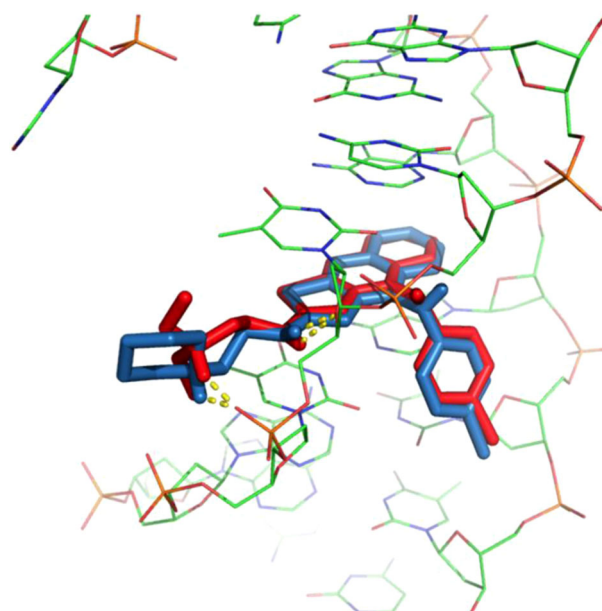


Fig. 4 Predicted docking geometries for compounds **15f** (blue) and **6c** (red). The theoretical hydrogen bonds are shown in yellow (Color figure online)

this substituent were shifted towards thymine ring, thus decreasing their overlap (Fig. 6). Formation of a charge transfer complex through π - π interactions is known to play a major role in the stability of DNA-intercalator complexes, and such electronic interaction depends on a good overlap. This observation can explain why the presence of a methylthio group at position 2 led to a reduction of the Q_{50} (increase in affinity). The reduction on the number of sites occupied by these derivatives in the DNA (Q_{\max}) relates with the ability of the compound to displace ethidium bromide from specific DNA sites, and cannot be directly correlated with the theoretical calculations presented here.

Molecular electrostatic potential (MEP) profiles

The above theoretical calculation depends on a force-field energy estimate. To take into account the electronic effects in the interaction energy, all-atom semiempirical QM calculations of the DNA-DNA intercalator complex were performed for selected compounds. The docking geometries were first refined through a PM7 geometry optimization, and then the enthalpy of formation of the complex was calculated as the difference of the complex energy minus the sum of the energies of the isolated molecules (in the same conformation). The resulting energy values are included in the Table 3. Direct comparison of the two estimates for the binding energy cannot be done, because the methods have a different level of theory, and because the QM calculation does not provide information on the entropic contribution to the complex stability. However, the

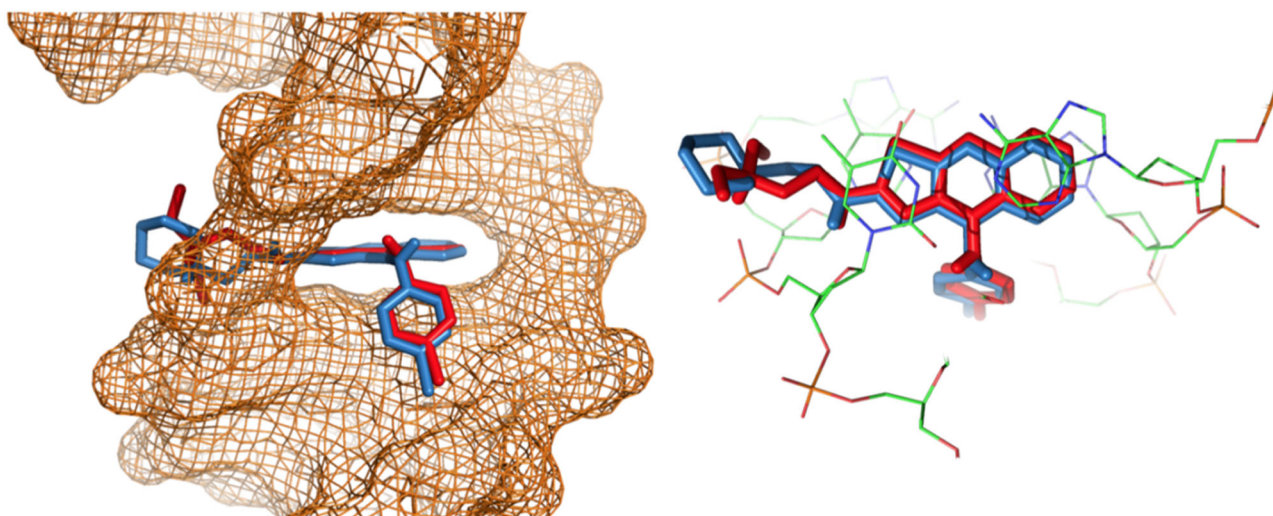
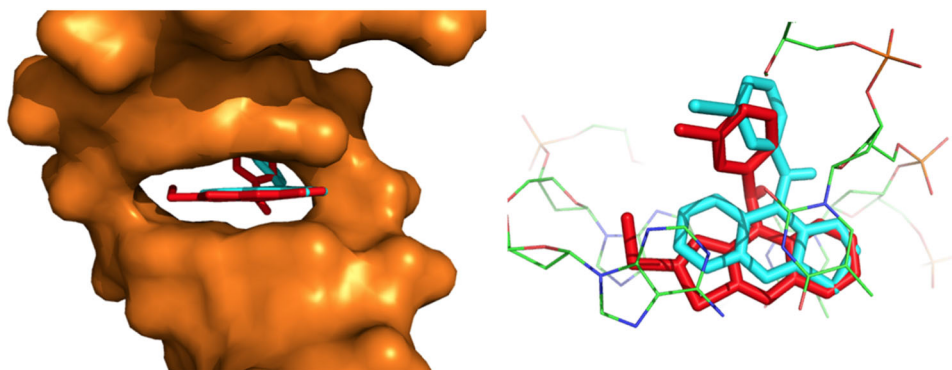


Fig. 5 *Left*, predicted binding geometries of compounds **15f** (blue) and **6c** (red) in DNA suggest intercalation as the dominant binding mode. The anilino group was found at the minor groove. *Right*, top view of

the DNA-thiazoloquinoline intercalation complex showing the maximum overlap with base pairs (Color figure online)

Fig. 6 *Left*, predicted binding geometries of compounds **16c** (cyan) and **13c** (red) in the DNA, showing intercalation as binding mode. *Right*, compound **13c** (red) intercalates with maximum overlap with base pairs (Color figure online)



results indicate a destabilization effect of anchoring the tertiary amine on the substituent at the 2-position (Table 3, **6c** vs. **15f**). In agreement with a more extensive overlap between the intercalator and the neighboring bases, the presence of the methylthio substituent at position 2 increases the stability of the complex. In addition, in all cases the LUMO orbital was localized on the thiazoloquinoline core (Fig. 7).

The introduction of an electron-withdrawing group on the anilino group decreases the LUMO energy values as demonstrated in Table 4 for compounds **6b**, **6c**, **15b**, **15c**, **15e** and **15f**. This trend correlates with cytotoxic activity and it is in excellent agreement with our previous results (Loza-Mejía et al., 2009). The same electronic trend is observed for compounds **13b**, **13c**, **16b** and **16c**, but the low or null cytotoxic activity of these compounds denotes that the presence of an aliphatic tertiary amine at 2-position is a relevant factor for the cytotoxic activity.

Previous studies have provided evidence of electrostatic factors as significant contributors to intercalation energy (Medhi et al., 1999; Bondarev et al., 2000). To evaluate how electrostatics may contribute to the observed biological differences between compounds of series **15** and **16**, electrostatic potential maps of DNA and thiazoloquinoline derivatives were calculated. A negatively charged surface is formed by the oxygen atoms of A617, A618, T619 and T620 (Fig. 8a). Compounds with a side chain at 2-position of the tricyclic system were predicted to orient this substituent towards this zone (Fig. 8b), which is expected to maximize electrostatic interactions between the cation and the DNA phosphates, particularly T619 and T620. In the case of compounds of series **16** the positively charged zone is located on the tertiary amine of position 2 (Fig. 8c), in accordance with the orientation of the intercalator in the predicted binding mode.

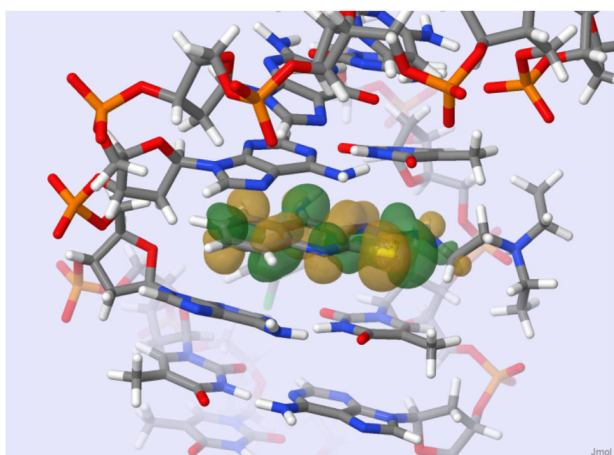


Fig. 7 A 3D view of the LUMO orbital for complex DNA-Compound **6c**. The positive or the negative sign of the wave function is indicated by the *green* or *golden color*, respectively (Color figure online)

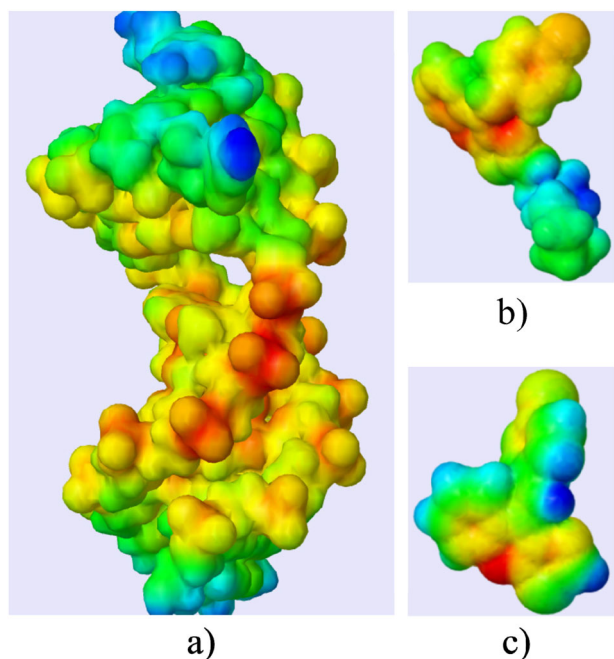


Fig. 8 Electrostatic potential surface maps of DNA **a**, compound **15f** **b** and compound **16c** **c** mapped on the total electron density calculated with PM7. *Red color* denotes the negative electrostatic potential and *blue color* denotes positive electrostatic potential (Color figure online)

Conclusion

The present study reveals a strong influence of the substitution pattern at the 2-position of the thiazolo[5,4-*b*]quinoline derivatives on the cytotoxic activity. This substitution pattern also has a significant influence on the intercalating properties of these compounds. The removal of

Table 4 PM7 calculated energy of the frontier orbitals (eV) for DNA bases and thiazolo[5,4-*b*]quinoline derivatives

Compound	A606 HOMO	A605 HOMO	T620 HOMO	T619 HOMO	Compound LUMO
6a	-8.5396	-8.5133	-8.5619	-8.8068	-0.5931
6b	-8.5996	-8.5410	-8.7457	-8.7884	-0.6868
6c	-8.4597	-8.5300	-8.8322	-8.8205	-0.6919
13a	-8.3603	-8.5435	-8.7015	-8.8130	-0.4837
13b	-8.3410	-8.6618	-8.5177	-8.8674	-0.8177
13c	-8.5907	-8.5617	-8.6701	-8.7833	-0.8862
15a	-8.6490	-8.5540	-8.7308	-8.7126	-0.7260
15b	-8.5818	-8.5333	-8.8000	-8.6712	-0.7033
15c	-8.4977	-8.2012	-8.5703	-8.8382	-0.7446
15d	-8.6429	-8.5067	-8.9088	-8.8246	-0.8684
15e	-8.5502	-8.5145	-8.7888	-8.7512	-0.7169
15f	-8.3681	-8.5360	-8.7800	-8.7182	-0.6182
16a	-8.5508	-8.5444	-8.7100	-8.8046	-0.6920
16b	-8.5193	-8.5100	-8.7355	-8.7257	-0.7475
16c	-8.5355	-8.5425	-8.7429	-8.7859	-0.8581
16d	-8.4989	-8.5384	-8.7459	-8.8601	-0.7260
16e	-8.5204	-8.4574	-8.6691	-8.8775	-0.4956
16f	-8.5543	-8.4890	-8.7466	-8.8178	-0.7387
16g	-8.5882	-8.5723	-8.7561	-8.7926	-1.0184
16h	-8.4675	-8.4640	-8.6772	-8.8169	-0.4545
16i	-8.6103	-8.5457	-8.7061	-8.7459	-0.6459

the methylthio group improves the intercalation of the derivatives into the DNA, but it does not render the compounds cytotoxic. The present study benefits from recent improvements in the semiempirical QM calculations to predict reliable geometries for macromolecular complexes and exploits the ability of these methods to estimate the influence of electronic effects in the binding mode of small molecules to biological macromolecules.

Experimental

Chemistry

All starting materials were commercially available research-grade chemicals and used without further purification. Reactions were monitored by analytical TLC on precoated silica gel 60 F₂₅₄ plates (Aldrich). Column chromatography was carried out on silica gel 60 (70–230 mesh, Merck). Melting points were determined on a Fisher-Jones apparatus and are uncorrected. Infrared spectra were recorded on a Nicolet FT-5SX spectrophotometer model. ¹H NMR spectra were recorded on a Varian VxR-300S spectrometer (300 MHz). Chemical shifts are reported in ppm (δ) and the

signals are described as singlet (s), doublet (d), triplet (t), quartet (q), broad (br) and multiplet (m); coupling constants are reported in Hz. EI-MS were carried out on a JEOL JMS-AX505-HA apparatus. FAB-MS were carried out on a JEOL Sx102 apparatus. Compounds **10–13** were prepared according to procedures already described.¹² (Loza-Mejía et al., 2009)

General preparation of 2-methylsulfonyl derivatives (series 14)

To a stirred suspension of 1.2 mmol of the 2-(methylthio)-9-anilinothiazolo[5,4-*b*]quinoline derivative with the desired substitution pattern in the aniline ring, in 5 mL of glacial acetic acid, 20 mg of Na₂WO₄•2H₂O were added. The resulting mixture was stirred for five minutes. Then 3 mL of hydrogen peroxide 30 % were dropwise in ten minutes. The reaction mixture was vigorously stirred for 30 min at room temperature. The suspension was poured over 50 mL of water under continuous stirring. The solids formed were collected by filtration, washed with water for several times, dried by suction and used without further purification.

General preparation of compounds 15a–15f

To a suspension of the corresponding 2-methylsulfonyl derivative **14** (0.6 mmol) in DMF (5 mL) at room temperature, the corresponding amine (1.6 mmol) was added dropwise. The suspension was stirred for 1 h at the same temperature and then poured over 50 mL of crushed ice/water. The precipitates formed were collected by filtration, washed with water and dried by suction. The residue was purified by column chromatography on silica gel using chloroform/methanol (9:1) as the eluent to afford the corresponding product.

N⁹-phenyl-N²-(2-(pyrrolidin-1-yl)ethyl)thiazolo[5,4-*b*]quinoline-2,9-diamine (**15a**)

Yellow solid (120 mg, 53.8 %), mp 89–90 °C; IR (KBr) cm⁻¹: 3413 (–NH–arom.), 3112–3063 (–CH insatd.), 2962–2919 (–CH satd.), 1476, 1536, 1577 (arom.), 756 (C–S); ¹H NMR (300 MHz, DMSO-*d*₆): δ = 8.56 (1H, s, Ar–N–H), 8.41 (1H, t, *J* = 6 Hz, aliph. N–H), 8.05 (1H, d, *J* = 6 Hz, H-5), 7.85 (1H, d, *J* = 6 Hz, H-8), 7.55 (1H, t, *J* = 6 Hz, H-7), 7.41 (1H, t, *J* = 9 Hz, H-6), 7.14 (2H, t, *J* = 9 Hz, H-2', H-6'), 6.76–6.86 (3H, dd, *J* = 9, 1.2 Hz, H-3', H-4', H-5'), 2.61 (2H, t, *J* = 6 Hz, NH–CH₂CH₂N(CH₂CH₂)₂), 3.29–3.46 (6H, m, NH–CH₂CH₂N(CH₂CH₂)₂), 1.66 (4H, br, NH–CH₂CH₂N(CH₂CH₂)₂). HRMS (FAB) calcd for [MH]⁺ C₂₂H₂₄N₅S: 390.18, found 390.1737; MS (FAB) *m/z*, rel. abundance %: 390 (MH⁺, 100 %), 389 (M⁺, 10 %),

305 (M⁺–84, 5 %), 154 (M⁺–235, 65 %), 84 (M⁺–305, 42 %).

N⁹-(3-chlorophenyl)-N²-(2-(pyrrolidin-1-yl)ethyl)thiazolo[5,4-*b*]quinoline-2,9-diamine (**15b**)

Yellow light solid (135 mg, 53.1 %), mp 109–111 °C; IR (KBr) cm⁻¹: 3373 (–NH– arom.), 3186 (–NH– aliph.), 3066 (–CH insatd.), 2997 (–CH satd.), 845 (–C–Cl), 759 (–C–S); ¹H NMR (300 MHz, DMSO-*d*₆): δ = 9.0 (1H, s, ArN–H), 8.73 (1H, br, aliph. N–H), 8.19 (1H, d, *J* = 6 Hz, H-5), 7.92 (1H, d, *J* = 6 Hz, H-8), 7.64 (1H, t, *J* = 6 Hz, H-7), 7.525 (1H, t, *J* = 6 Hz, H-6), 7.21 (1H, t, *J* = 9 Hz, H-6'), 6.76–6.87 (3H, m, H-2', H-3', H-4'), 2.91 (2H, s, NH–CH₂CH₂N(CH₂CH₂)₂), 2.75 (2H, s, NH–CH₂CH₂N(CH₂CH₂)₂), 2.525 (4H, br, NH–CH₂CH₂N(CH₂CH₂)₂), 1.79 (4H, br, NH–CH₂CH₂N(CH₂CH₂)₂); HRMS (FAB) calcd for [MH]⁺ C₂₂H₂₃N₅ClS: 424.14, found 424.1365; MS (FAB) *m/z*: 424 (MH⁺, 43 %), 426 (MH⁺+2, 16 %, ³⁷Cl and ³⁴S): 423 (M⁺, 5 %), 154 (M⁺–269, 100 %), 136 (M⁺–287, 66 %), 84 (M⁺–339, 17 %).

N⁹-(4-chlorophenyl)-N²-(2-(pyrrolidin-1-yl)ethyl)thiazolo[5,4-*b*]quinoline-2,9-diamine (**15c**)

Yellow light solid (150 mg, 62.4 %), mp 85–86 °C; IR (KBr) cm⁻¹: 3236 (–NH– arom.), 3029 (–NH aliph.), 2956 (–CH insatd.), 2818 (–CH satd.), 1672 (C=N), 1559, 1523, 1490 (arom.) 851 (C–Cl), 761 (–C–S); ¹H NMR (300 MHz, DMSO-*d*₆): δ = 8.74 (1H, s, ArN–H), 8.42 (1H, t, *J* = 5.1 Hz, aliph. N–H), 8.13 (1H, dd, *J* = 1.2, 8.7 Hz, H-5), 7.85 (1H, dd, *J* = 9.6, 0.1 Hz, H-8), 7.56 (1H, ddd, *J* = 1.2, 6.9, 9.6 Hz, H-7), 7.44 (1H, ddd, *J* = 1.2, 6.9, 8.4 Hz, H-6), 7.15 (2H, d, *J* = 8.7 Hz, H-3' and H-5'), 6.78 (2H, d, *J* = 8.7 Hz, H-2' and H-6'), 2.87 (2H, s, NH–CH₂CH₂N(CH₂CH₂)₂), 2.72 (2H, s, NH–CH₂CH₂N(CH₂CH₂)₂), 2.36 (4H, br, NH–CH₂CH₂N(CH₂CH₂)₂), 1.61–1.64 (4H, m, NH–CH₂CH₂N(CH₂CH₂)₂). HRMS (FAB) calcd for [MH]⁺ C₂₂H₂₃N₅ClS: 424.14, found 424.1364; MS (FAB) *m/z*: 424 (MH⁺, 100 %), 426 (MH⁺+2, 38 %, ³⁷Cl and ³⁴S), 423 (M⁺, 14 %), 154 (M⁺–269, 66 %), 84 (M⁺–339, 76 %).

N⁹-phenyl-N²-(2-(piperidin-1-yl)ethyl)thiazolo[5,4-*b*]quinoline-2,9-diamine (**15d**)

Yellow light solid (180 mg, 68.5 %), mp 80–82 °C; IR (KBr) cm⁻¹: 3239 (–NH–arom.), 3191 (–NH–aliph.), 3052 (–CH insatd.), 2852 (–CH satd.), 1588 (C=N), 1523, 1493, 1434 (aromatic), 759 (–C–S); ¹H NMR (300 MHz, DMSO-*d*₆): δ = 8.61 (1H, s, ArN–H), 8.45 (1H, br, aliph. N–H), 8.10 (1H, d, *J* = 6 Hz, H-5), 7.86 (1H, d, *J* = 9 Hz, H-8), 7.6 (1H, t, *J* = 6 Hz, H-6), 7.42 (1H, t, *J* = 9 Hz, H-7), 7.16 (2H, t, *J* = 9 Hz, H-2', H-6'), 6.81 (3H, t, *J* = 9 Hz, H-3', H-4', H-5'),

2.49 (2H, t, $J = 3$ Hz, $\text{NH}-\text{CH}_2\text{CH}_2\text{N}(\text{CH}_2\text{CH}_2)_2\text{CH}_2$), 3.30–3.38 (6H, m, $\text{NH}-\text{CH}_2\text{CH}_2\text{N}(\text{CH}_2\text{CH}_2)_2\text{CH}_2$), 1.46–1.58 (4H, br, $\text{NH}-\text{CH}_2\text{CH}_2\text{N}(\text{CH}_2\text{CH}_2)_2\text{CH}_2$), 1.33–1.43 (2H, br, $\text{NH}-\text{CH}_2\text{CH}_2\text{N}(\text{CH}_2\text{CH}_2)_2\text{CH}_2$). HRMS (FAB) calcd for $[\text{MH}]^+ \text{C}_{23}\text{H}_{26}\text{N}_5\text{S}$: 404.19, found 404.1911; MS (EI) m/z : 403 (M^+ , 4%), 401 (M^+-2 , 2%), 305 (M^+-98 , 10%), 292 (M^+-111 , 34%), 111 (M^+-292 , 68%), 98 (M^+-305 , 100%).

N^9 -(3-chlorophenyl)- N^2 -(2-(piperidin-1-yl)ethyl)thiazolo[5,4-b]quinoline-2,9-diamine (**15e**)

Yellow light solid (153 mg, 58.5%), mp 95–96 °C; IR (KBr) cm^{-1} : 3213 (–NH–arom.), 3058 (–NHR), 2933 (–CH insatd.), 2852, 2804 (–CH satd.), 1594, 1666 (–C=N), 1560, 1477, 1441 (arom.), 855 (–C–Cl), 759 (–C–S); ^1H NMR (300 MHz, $\text{DMSO}-d_6$): $\delta = 8.84$ (1H, s, ArN–H), 8.41 (1H, br, aliph. N–H), 8.11 (1H, d, $J = 6$ Hz, H-5), 7.875 (1H, d, $J = 6$ Hz, H-8), 7.58 (1H, 1H, $J = 6.9$ Hz, H-6), 7.7 (1H, t, $J = 6.9$ Hz, H-7), 7.14 (1H, t, $J = 9$ Hz, H-6'), 6.70–6.79 (3H, m, H-2', H-3', H-4'), 2.49 (2H, br, $\text{NH}-\text{CH}_2\text{CH}_2\text{N}(\text{CH}_2\text{CH}_2)_2\text{CH}_2$), 2.40 (2H, br, $\text{NH}-\text{CH}_2\text{CH}_2\text{N}(\text{CH}_2\text{CH}_2)_2\text{CH}_2$), 2.27 (4H, br, $\text{NH}-\text{CH}_2\text{CH}_2\text{N}(\text{CH}_2\text{CH}_2)_2\text{CH}_2$), 1.44 (4H, br, $\text{NH}-\text{CH}_2\text{CH}_2\text{N}(\text{CH}_2\text{CH}_2)_2\text{CH}_2$), 1.35 (2H, br, $\text{NH}-\text{CH}_2\text{CH}_2\text{N}(\text{CH}_2\text{CH}_2)_2\text{CH}_2$). HRMS (FAB) calcd for $[\text{MH}]^+ \text{C}_{23}\text{H}_{25}\text{N}_5\text{ClS}$: 438.152, found 438.1522; MS (FAB) m/z : 438 (MH^+ , 88%), 440 (MH^++2 , 31%, ^{37}Cl and ^{34}S), 437 (M^+ , 16%), 436 (MH^+-2 , 15%), 435 (M^+-2 , 4%), 326 (M^+-111 , 6%), 111 (M^+-326 , 50%), 98 (M^+-339 , 100%).

N^9 -(4-chlorophenyl)- N^2 -(2-(piperidin-1-yl)ethyl)thiazolo[5,4-b]quinoline-2,9-diamine (**15f**)

Yellow light solid (148 mg, 67.6%), mp 140–141 °C; IR (KBr) cm^{-1} : 3373 (–NH–arom.), 3057 (–NH aliph.), 2928 (–CH insatd.), 2851, 2797 (–CH satd.), 1694, 1605 (–C=N), 1557, 1493, 1469 (arom.), 855 (–C–Cl), 759 (–C–S); ^1H NMR (300 MHz, $\text{DMSO}-d_6$): $\delta = 8.8$ (1H, s, ArN–H), 8.38 (1H, t, $J = 6$ Hz, aliph. N–H), 8.15 (1H, d, $J = 9$ Hz, H-5), 7.9 (1H, d, $J = 9$ Hz, H-8), 7.6 (1H, ddd, $J = 1.2, 7.2, 8.1$ Hz, H-7), 7.49 (1H, ddd, $J = 1.2, 6.9, 8.1$ Hz, H-6), 7.25 (2H, d, $J = 9$ Hz, H-3', H-5'), 6.8 (2H, d, $J = 9$ Hz, H-2', H-6'), 2.53 (2H, q, $J = 6.3$ Hz, $\text{NH}-\text{CH}_2\text{CH}_2\text{N}(\text{CH}_2\text{CH}_2)_2\text{CH}_2$), 2.39 (2H, t, $J = 6$ Hz, $\text{NH}-\text{CH}_2\text{CH}_2\text{N}(\text{CH}_2\text{CH}_2)_2\text{CH}_2$), 2.28 (4H, br, $\text{NH}-\text{CH}_2\text{CH}_2\text{N}(\text{CH}_2\text{CH}_2)_2\text{CH}_2$), 1.475 (4H, br, $\text{NH}-\text{CH}_2\text{CH}_2\text{N}(\text{CH}_2\text{CH}_2)_2\text{CH}_2$), 1.39 (2H, br, $\text{NH}-\text{CH}_2\text{CH}_2\text{N}(\text{CH}_2\text{CH}_2)_2\text{CH}_2$). HRMS (FAB) calcd for $[\text{MH}]^+ \text{C}_{23}\text{H}_{25}\text{N}_5\text{ClS}$: 438.15, found 438.1522; MS (FAB) m/z : 438 (MH^+ , 100%), 440 (MH^++2 , 38%, ^{37}Cl and ^{34}S), 437 (M^+ , 18%), 326 (M^+-111 , 6%), 111 (M^+-326 , 40%), 98 (M^+-339 , 88%).

General preparation of compounds 16a–16i

To a stirred suspension of the corresponding 2-methylsulfanyl derivative **14** (0.62 mmol) in absolute ethanol (6 mL) at room temperature, 5 mg (0.14 mmol) of NaBH_4 were added. The reaction mixture was stirred for 24 h at room temperature. The final solution was acidified with 2 mL HCl 10% (v/v). The precipitates formed were collected by filtration, washed with a saturated aqueous NaHCO_3 solution and water. The residue was purified by column chromatography on silica gel using dichloromethane/methanol (9:1) as the eluent to afford the corresponding product.

N -phenylthiazolo[5,4-b]quinolin-9-amine (**16a**)

Yellowish solid (130 mg, 75%), mp 135 °C; IR (KBr) cm^{-1} : 3413 (–NH–aromatic), 3212–2924 (–CH insatd.), 1710, 1536, 1577 (aromatic), 1495, 756 (C–S). No bands at 1317 and 1146, typical for sulfonyl group. ^1H NMR (300 MHz, $\text{DMSO}-d_6$): $\delta = 9.46$ (1H, s, ArN–H), 9.20 (1H, s, H-2), 8.34 (1H, dd, $J = 8.3, 0.8$ Hz, H-8), 7.98 (1H, ddd, $J = 8.7, 1.4, 0.6$ Hz, H-5), 7.76 (1H, ddd, $J = 8.4, 6.7, 1.4$ Hz, H-6), 7.50 (1H, ddd, $J = 8.5, 6.7, 1.3$ Hz, H-7), 7.25–7.22 (2H, m, H, 3', H-5'), 7.10–7.04 (2H, m, H-2', H-6'), 7.04–6.96 (1H, m, H-4'). HRMS (ESI) calcd for $[\text{M}]^+ \text{C}_{16}\text{H}_{11}\text{N}_3\text{S}$: 277.07, found: 277.0672; MS (FAB) m/z : 277 (MH^+ , 100%).

N -(3-chlorophenyl)thiazolo[5,4-b]quinolin-9-amine (**16b**)

Yellow light solid (140 mg, 79%), mp 160 °C; IR (KBr) cm^{-1} : 3402, 3354 (–NH aromatic), 3045, 1589, 1517, 1431, 830, 761; ^1H NMR (300 MHz, $\text{DMSO}-d_6$): $\delta = 9.62$ (1H, s, ArN–H), 9.2 (1H, s, H-2), 8.45 (1H, d, $J = 8.4$ Hz, H-8), 7.94 (1H, dd, $J = 8.4, 0.9$ Hz, H-5), 7.79 (1H, ddd, $J = 8.1, 6.6, 1.2$ Hz, H-6), 7.58 (1H, ddd, $J = 8.1, 6.6, 2.1$ Hz, H-7), 7.3 (1H, dd, $J = 8.1, 8.1$ Hz, H-5'), 7.18 (1H, dd, $J = 2.1, 2.1$ Hz, H-2'), 7.06 (1H, m, H-6'), 7.09 (1H, m, H-4'). HRMS (ESI) calcd for $[\text{M}]^+ \text{C}_{16}\text{H}_{10}\text{N}_3\text{ClS}$: 311.03, found: 311.0278; MS (FAB) m/z : 311 (MH^+ , 100%).

N -(4-chlorophenyl)thiazolo[5,4-b]quinolin-9-amine (**16c**)

Yellow solid, (135 mg, 76.8%), mp 180 °C; IR (KBr) cm^{-1} : 3399 (–NH arom.), 3051–2992 (–CH insatd.), 1580, 1513, 826 (C–Cl), 753; ^1H NMR (300 MHz, $\text{DMSO}-d_6$): $\delta = 9.54$ (1H, s, ArN–H), 9.22 (1H, s, H-2), 8.68 (1H, d, $J = 8.4$ Hz, H-8), 7.94 (1H, d, $J = 8.4$ Hz, H-5), 7.91 (1H, dd, $J = 7.9$ Hz, H-6), 7.6 (1H, dd, $J = 7.6$ Hz, H-7), 7.4 (2H, d, $J = 8.8$ Hz, H-3', H-5'), 7.3 (2H, d, $J = 8.4$ Hz, H-2', H-6'). HRMS

(ESI) calcd for $[M]^+$ $C_{16}H_{10}N_3ClS$: 311.03, found: 311.0277; MS (FAB) m/z : 311 (M^+ , 100 %).

N-(3-methoxyphenyl)thiazolo[5,4-*b*]quinolin-9-amine (**16d**)

Yellow solid (137 mg, 72 %), mp 151 °C; IR (KBr) cm^{-1} : 3120 (–NH arom.), 3053–3013 (–CH insatd.), 2966 1595, 1571, 1543, 1503, 1476 (arom), 1266 (Ar–O), 764; 1H NMR (300 MHz, DMSO- d_6): δ = 9.4 (1H, s, –NH–Ar), 9.22 (1H, s, H-2), 8.29 (1H, d, J = 8.4 Hz, H-8), 7.97 (1H, dd, J = 8.7, 0.9 Hz, H-5), 7.75 (1H, ddd, J = 8.4, 6.9, 1.2 Hz, H-6), 7.49 (1H, ddd, J = 8.4, 6.9, 1.2 Hz, H-7), 7.11 (1H, t, J = 8.7 Hz, H-5'), 6.60–6.58 3H, (m, 3H, H-2', H-4', H-6'), 3.65 (3H, s, –OCH₃). ^{13}C NMR (75 MHz, DMSO- d_6): δ 160.7 (C-2), 141.1 (C-3a), 144.7 (C-4a), 128.7 (C-5), 130.2 (C-6), 124.7 (C-7), 124.4 (C-8), 119.5 (C-8a), 160 (C-9), 133.1 (C-9a), 148.1 (C-1'), 106.5 (C-2'), 153.2 (C-3'), 108.2 (C-4'), 129.5 (C-5'), 113.1 (C-6'), 55.3, (–OCH₃). HRMS (ESI) calcd for $[M]^+$ $C_{17}H_{13}ON_3S$: 307.08, found: 307.078; MS (EI) m/z : 307 (M^+ , 100 %), 292 (M^+ –15, 78 %).

N-(4-methoxyphenyl)thiazolo[5,4-*b*]quinolin-9-amine (**16e**)

Yellow solid (140 mg, 70 %), mp 147; IR (KBr) cm^{-1} : 3120 (NH– arom.), 3053–2966 (–CH insatd.), 1595, 1571, 1543, 1503, 1476 (arom.), 1244 (Ar–O), 1041 (Ar–O–CH₃), 752 (C–S); 1H NMR (300 MHz, DMSO- d_6): δ = 9.29 (1H, s, –NH–Ar), 9.07 (1H, s, H-2), 8.31 (1H, d, J = 8.4 Hz, H-8), 7.9 (1H, dd, J = 8.4 Hz, H-5), 7.7 (1H, ddd, J = 7.6 Hz, H-6); 7.42 (1H, dd, J = 7.6 Hz, H-7), 7.06 (1H, d, J = 8.4 Hz, H-2'), 6.85 (3H, d, J = 8.4 Hz, H-3', H-5', H-6'), 3.73 (3H, s, –OCH₃). HRMS (ESI) calcd for $[M]^+$ $C_{17}H_{13}ON_3S$: 307.08, found: 307.0772; MS (EI) m/z : 307 (M^+ , 100 %), 292 (M^+ –15, 80 %).

N-(3-cyanophenyl)thiazolo[5,4-*b*]quinolin-9-amine (**16f**)

Yellow solid (135 mg, 77.3 %), mp 160 °C; IR (KBr) cm^{-1} : 3329 (–NH arom.), 3056–2923 (–CH insatd.), 2231 (–CN), 1578, 1548, 1533 (arom.), 757 (C–S); 1H NMR (300 MHz, DMSO- d_6): δ = 9.7 (1H, s, ArN–H), 9.3 (1H, s, H-2), 8.64 (1H, d, J = 8.7 Hz, H-8), 8.0 (1H, dd, J = 8.7, 0.9 Hz, H-5), 7.89 (1H, ddd, J = 8.4, 6.9, 1.2 Hz, H-6), 7.68 (1H, ddd, J = 8.4, 6.9, 1.2 Hz, H-7), 7.56–7.46 (4H, m, H-2', H-4', H-5', H-6'). HRMS (ESI) calcd for $[M]^+$ $C_{17}H_{10}N_4S$: 302.06, found: 302.0615; MS (EI) 302 M^+ .

N-(4-cyanophenyl)thiazolo[5,4-*b*]quinolin-9-amine (**16g**)

Yellow solid (142 mg, 80 %), mp 162 °C; IR (KBr) cm^{-1} : 3320 (–NH–arom.), 3055–2923 (–CH insatd.), 2219 (–CN), 1607, 1578, 1524, 1405 (arom.), 753 (–C–S); 1H NMR

(300 MHz, DMSO- d_6): δ = 9.6 (1H, s, Ar–NH–), 9.3 (1H, s, H-2), 8.5 (1H, d, J = 8.4 Hz, H-8), 8.0 (1H, d, J = 8.4 Hz, H-5), 7.8 (1H, dd, J = 7.2 Hz, H-6), 7.7 (2H, d, J = 8.8 Hz, H-3', H-5'), 7.6 (1H, dd, J = 7.2 Hz, H-7), 7.2 (2H, d, J = 8.4 Hz, H-2', H-6'). HRMS (ESI) calcd for $[M]^+$ $C_{17}H_{10}N_4S$: 302.06, found: 302.0619; MS (EI) 302 M^+ .

N-(3-methylphenyl)thiazolo[5,4-*b*]quinolin-9-amine (**16h**)

Yellow solid, (150 mg, 79 %), mp 132 °C; IR (KBr) cm^{-1} : 3120 (NH arom.), 3068–2911 (–CH insatd.), 1595, 1571, 1543, 1503, 1476 (arom.), 753 (C–S); 1H NMR (300 MHz, DMSO- d_6): δ = 9.35 (1H, s, –NH–Ar), 9.18 (1H, s, H-2), 8.29 (1H, d, J = 8.4 Hz, H-8), 7.95 (1H, dd, J = 8.7, 0.9 Hz, H-5), 7.73 (1H, ddd, J = 8.4, 6.9, 1.2 Hz, H-6), 7.47 (1H, ddd, J = 8.4, 6.9, 1.2 Hz, H-7), 7.1 (1H, t, J = 8.6 Hz, H-5'), 6.86 (3H, m, H-2', H-4', H-6'), 2.21 (3H, s, Ar–CH₃). HRMS (ESI) calcd for $[M]^+$ $C_{17}H_{13}N_3S$: 291.03, found: 291.0813; MS (EI) m/z : 291 (M^+ , 100 %), 290 (M^+ –1, 75 %).

N-(4-methylphenyl)thiazolo[5,4-*b*]quinolin-9-amine (**16i**)

Yellow solid (145 mg, 76 %) mp 196 °C; IR (KBr) cm^{-1} : 3120 (NH arom.), 3048–2941 (–CH arom.), 1595, 1571, 1543, 1503, 1476 (arom.), 739 (C–S); 1H NMR (300 MHz, DMSO- d_6): δ = 9.34 (1H, s, –NH–Ar), 9.14 (1H, s, H-2), 8.3 (1H, d, J = 8.4 Hz, H-8), 7.93 (1H, dd, J = 8.7, 0.9 Hz, H-5), 7.72 (1H, ddd, J = 8.4, 6.9, 1.2 Hz, H-6), 7.45 (1H, ddd, J = 8.4, 6.9, 1.2 Hz, H-7), 7.05 (2H, d, J = 8.6 Hz, H-2', H-6'), 6.97 (2H, d, J = 8.6 Hz, H-3', H-5'), 2.26 (3H, s, Ar–CH₃). HRMS (ESI) calcd for $[M]^+$ $C_{17}H_{13}N_3S$: 291.03, found: 291.0825; MS (EI) m/z : 291 (M^+ , 100 %), 290 (M^+ –1, 75 %).

Biological

Cytotoxic assay

The effects of the compounds were determined in one cervical cell line (HeLa), two human colorectal cancer cell lines (SW480 and SW620) and one myelogenous leukemia human cell line (K-562). The cytotoxic assays were carried out according to the microculture MTT method (Quintero et al., 1999). The cells were harvested at 4.5 – 5.0×10^4 cells/mL/well and inoculated on 24 well microtiter plates. Then the culture cells were inoculated alone and with the compounds (which were dissolved in DMSO and added in a maximum volume of 2 mL/mL/well). After 72 h incubation, 100 mg/mL of MTT (in PBS, pH 7.2) were added. By adding 1 mL of DMSO to each well, followed by gentle shaking, the formazan dye was dissolved. After centrifugation the extinction coefficient was measured at 540

nm using a Beckman photometer model DUR-64. Cell growth inhibition was determined by the formula % cell growth inhibition = $(1 - \text{absorbance of treated cells} / \text{absorbance of untreated cells}) \times 100$. The assays were carried out in three independent experiments in quadruplicate.

DNA affinity and intercalation

DNA intercalation was determined from the displacement of ethidium bromide from DNA (Loza-Mejía et al., 2008). Sterile solutions of high molecular weight DNA from calf thymus (Gibco, BRL, New York, USA) in a 0.1 M Tris-HCl buffer at pH 7.4, 0.15M NaCl and 5 mM ethidium bromide (ultrapure from Gibco, BRL, New York, USA) were mixed with serial additions of the compounds to be tested dissolved in 100 % dimethylsulphoxide (DMSO); the fluorescence intensity of the solution was recorded at 584 nm with an excitation light of 546 nm. The DMSO concentration never exceeded 8 %. The effect of this amount of DMSO was small and had no effect on the shape of emission or excitation fluorescence spectra of a DNA-ethidium bromide complex as compared with that determined in 100 % aqueous buffers. The recorded fluorescence change was corrected for the dilution caused by serial additions of this solvent. The concentration of the compounds tested varied in the range of 1–100 μM depending on their respective solubility. The precipitation of the compound from the solution was detected from an increase in 600 nm light dispersal at 90° in a Shimadzu RF5000U fluorescence spectrophotometer. The displacement curves were fitted by non-linear regression analysis to a rectangular hyperbola.

Molecular docking

The crystal structure of an 9-acridine-peptide drug in complex with a DNA dodecamer was downloaded from Protein Data Bank (PDB ID: 1G3X) (Malinina et al., 2002) and edited using PyMOL v.1.4.1 software (<http://www.pymol.org>), after edition the structure was minimizing with WHAT IF: A molecular modeling and drug design program (<http://swift.cmbi.ru.nl/whatif/>) (Vriend, 1990) and ready for docking studies. All docking studies were performed with AutoDock 4.2. software (Morris et al., 1996, 1998) employing the Lamarckian Genetic Algorithm, generating 20 independent docking poses for each compound. In all the cases the population size was set to 150 and the maximal number of evaluations was set to 5,000,000. The position of the docking grid was centered at the position of the original co-crystallized ligand which was removed. The dimension of the grid was 100 Å \times 100 Å \times 100 Å points with spacing of 0.375 between the grid points. The DNA was considered as rigid molecule, while the ligands were considered as flexible molecules. The best binding mode was selected

based on the lowest binding free energy and the largest cluster size.

Ligands equilibrium geometries. All calculations were performed with SPARTAN'08® software (2008, WAVE-FUNCTION, Inc., Irvine, CA). Molecules were built by assembling standard fragments and the resulting geometries were optimized by molecular mechanics. Conformational analysis of the compounds by Systematic Search protocol around rotatable bonds was performed using the MMFF94 force field. The most frequent conformer for each compound was selected and geometry optimization was carried out with semiempirical AM1 method. Due to the basic properties of the tertiary amino side chain at 2-position, the protonated form of the compounds with this substituent was used in the docking studies and neutral form was also used.

Semiempirical LMO calculations of DNA–DNA intercalator complexes

The representative geometry of selected DNA–DNA-intercalator complexes, obtained from the molecular docking predictions with the best score belonging to the largest cluster, was edited to add all missing hydrogen atoms with the phosphate groups unprotonated. MOPAC 2012 (Stewart, 2012; Maia et al., 2012) was used to improve the molecular geometry using the semiempirical PM7 method and the Localized Molecular Orbital theory as implemented in the MOPAC MOZYME code. Implicit solvation was set using the conductor-like screening model (COSMO) with a dielectrical constant of 78.4 in a non-periodical box and in the absence of other explicit atoms, such as sodium ions. Geometry optimization was run in two steps, first heavy-atoms were fixed and hydrogen positions were optimized to a gradient of 20.0 kcal mol⁻¹ Å⁻¹. When required, anomalous hydrogen positions were corrected and the step was repeated. When a chemically consistent geometry for all hydrogen atoms was obtained a free optimization of all atoms was run to a gradient of 10.0 kcal mol⁻¹ Å⁻¹ (a recommended target for large systems). Analysis of molecular graphics was done using Jmol v. 13.0. (<http://www.jmol.org/>).

Acknowledgments We thank Maricela Gutiérrez, Rosa Isela del Villar, Victor M. Arroyo, Georgina Duarte and Margarita Guzmán for determination of all spectra. A.K.L.R. thanks DGAPA-UNAM for a scholarship. We also thank DGAPA-UNAM for financing project PAPIIT IN2128910 and PAPIIT IN221113, as well as Facultad de Química for financial support (PAIP 6390-10, 6290-09), and UNAM-DGTIC-SC16-1-IR-111.

Compliance with ethical standards

Conflict of interest The authors declare that they have no conflict of interests.

References

- Baldwin JJ, Engelhardt EL, Hirschmann R, Ponticello GS, Atkinson JG, Wasson BK, Sweet CS, Scriabine A (1980) Heterocyclic analogues of the antihypertensive beta-adrenergic blocking agent (S)-2-[3-(ter-butylamino)-2-hydroxypropoxy]-3-cyanopyridine. *J Med Chem* 23:65–70
- Bondarev DA, Skawinski WJ, Venanzi CA (2000) Nature of intercalator amiloride-nucleobase stacking. an empirical potential and ab initio electron correlation study. *J Phys Chem B* 104:815–822
- Chen Y-L, Chen I-L, Lu C-M, Tzeng C-C, Tsao L-T, Wang J-P (2004) Synthesis and anti-inflammatory evaluation of 4-anilino-furo[2,3-*b*]quinoline and 4-phenoxyfuro[2,3-*b*]quinoline derivatives. *Bioorg Med Chem* 12:387–392
- Chen Y-L, Chen I-L, Wang T-C, Han C-H, Tzeng C-C (2005) Synthesis and anticancer evaluation of certain 4-anilino-furo[2,3-*b*]quinoline and 4-anilino-furo[3,2-*c*]quinoline derivatives. *Eur J Med Chem* 40:928–934
- Demecunynck H, Charmantray F, Martelli A (2001) Interest of acridine derivatives in the anticancer chemotherapy. *Curr Pharm Des* 7:1703–1724
- Denny WA (1995) The role of intercalation and DNA binding in the activity of acridines and related tricyclic DNA-intercalating agents. In: Foye WO (ed) *Cancer chemotherapeutic agents*. ACS, Washington, pp 218–239
- Denny WA (2002) Acridine derivatives as chemotherapeutic agents. *Curr Med Chem* 9:1655–1665
- González-Sánchez I, Solano JD, Loza-Mejía MA, Olvera-Vázquez S, Rodríguez-Sotres R, Morán J, Lira-Rocha A, Cerbon M (2011) Antineoplastic activity of the thiazolo[5,4-*b*]quinoline derivative D3CLP in K-562 cells is mediated through effector caspases activation. *Eur J Med Chem* 46:2102–2108
- Gunawardana GP, Kohmoto S, Gunasekera SP, McConnell OJ, Koehn FE (1988) Dercitin, a new biologically active acridine alkaloid from a deep water marine sponge, *Dercitus* sp. *J Am Chem Soc* 110:4856–4860
- He Y, Ma X, Ji HF, Zha XB, Jiang H, Lu M (2012) Selective oxidation of sulfides to sulfoxides/sulfones by 30 % hydrogen peroxide. *Phosphorus Sulfur Silicon Relat Elem* 187:822–830
- Herrera A, Martínez-Alvarez R, Ramiro P, Molero D, Almy J (2006) New easy approach to the synthesis of 2,5-disubstituted and 2,4,5-trisubstituted 1,3-oxazoles. The reaction of 1-(methylthio) acetone with nitriles. *Org Chem* 71:3026–3032
- Hoelder S, Clarke PA, Workman P (2012) Discovery of small molecule cancer drugs: successes, challenges and opportunities. *Mol Oncol* 6:155–176
- Kerdesky FA, Seif LS (1995) A novel and efficient synthesis of 5-(hydroxymethyl) thiazole: an important synthon for preparing biologically active compounds. *Synth Commun* 25:2639–2645
- Lindsey RH, Pendleton M, Ashley RE, Mercer SL, Deweese JE, Osheroff N (2014) Catalytic core of human topoisomerase II α : insights into enzyme-DNA interactions and drug mechanism. *Biochemistry* 53:6595–6602
- Loza-Mejía MA, Maldonado-Hernández K, Rodríguez-Hernández F, Rodríguez-Sotres R, González-Sánchez I, Solano JD, Lira-Rocha A (2008) Synthesis, cytotoxic evaluation, and DNA binding of novel thiazolo[5,4-*b*]quinoline derivatives. *Bioorg Med Chem* 16:1142–1149
- Loza-Mejía MA, Olvera-Vázquez S, Maldonado-Hernández K, Guadarrama-Salgado K, González-Sánchez I, Rodríguez-Hernández F, Solano JD, Rodríguez-Sotres R, Lira-Rocha A (2009) Synthesis, cytotoxic activity, DNA topoisomerase-II inhibition, molecular modeling and structure-activity relationship of 9-anilinothiazolo[5,4-*b*]quinoline derivatives. *Bioorg Med Chem* 17:3266–3277
- Maia JDC, Carvalho GAU, Manguiera CP, Santana SR, Cabral LAF, Rocha GB (2012) GPU linear algebra libraries and GPGPU programming for accelerating MOPAC semiempirical quantum chemistry calculations. *J Chem Theory Comput* 8:3072–3081
- Malinina L, Soler-López M, Aymamí J, Subirana JA (2002) Intercalation of an acridine-peptide drug in an AA/TT base step in the crystal structure of [d(CGCGAATTCGCG)](2) with six duplexes and seven Mg(2⁺) ions in the asymmetric unit. *Biochemistry* 41:9341–9348
- Medhi C, Mitchell JBO, Price SL, Tabor AB (1999) Electrostatic factors in DNA intercalation. *Biopolymers* 52:84–93
- McConnaughie WA, Jenkins TC (1995) Novel acridine-triazenes as prototype combilexins: synthesis, DNA binding, and biological activity. *J Med Chem* 38:3488–3501
- Morris GM, Goodsell DS, Halliday RS, Huey R, Hart WE, Belew RK, Olson AJ (1998) Automated docking using a Lamarckian genetic algorithm and an empirical binding free energy function. *J Comput Chem* 19:1639–1662
- Morris GM, Goodsell DS, Huey R, Olson AJ (1996) Distributed automated docking of flexible ligands to proteins: parallel applications of AutoDock 2.4. *J Comput Aided Mol Des* 10:293–304
- Quintero A, Pelcastre A, Dolores J, Guzmán E, Díaz E (1999) Antitumoral activity of new pyrimidine derivatives of sesquiterpene lactones. *J Pharm Pharm Sci* 2:108–112
- Rodríguez-Loaiza P, Quintero A, Rodríguez-Sotres R, Solano JD, Lira-Rocha A (2004) Synthesis and evaluation of 9-anilinothiazolo[5,4-*b*]quinoline derivatives as potential antitumorals. *Eur J Med Chem* 39:5–10
- Sato K, Hyodo M, Aoki M, Zheng X-Q, Noyori R (2001) Oxidation of sulfides to sulfoxides and sulfones with 30 % hydrogen peroxide under organic solvent- and halogen-free conditions. *Tetrahedron* 57:2469–2476
- Stewart JJP MOPAC (2012) *Stewart Computational Chemistry*, Version 15.140L web: <http://OpenMopac.net>
- Siu F-M, Pommier Y (2013) Sequence selectivity of the cleavage sites induced by topoisomerase I inhibitors: a molecular dynamics study. *Nucleic Acid Res* 41:10010–10019
- Vriend G (1990) WHAT IF: a molecular modeling and drug design program. *J Mol Graph* 8:52–56
- Xiao X, Antony S, Pommier Y, Cushman M (2005) On the binding of indeno[1,2-*c*]isoquinolines in the DNA-topoisomerase I cleavage complex. *J Med Chem* 48:3231–3238
- Yin G, Wang Z, Chen A, Gao M, Wu A, Pan Y (2008) A new facile approach to the synthesis of 3-methylthio-substituted furans, pyrroles, thiophenes, and related derivatives. *J Org Chem* 73:3377–3383
- Zumbrunn A (1998) The first versatile synthesis of 1-alkyl-3-fluoro-1*H*-[1,2,4]triazoles. *Synthesis* 9:1357–1361